

The toposcopy, a new tool to probe the geometry of an irregular interface by measuring its transfer impedance

MARCEL FILOCHE^{1,2} AND DENIS S. GREBENKOV¹

¹*Physique de la Matière Condensée, Ecole Polytechnique, CNRS, 91128 Palaiseau, France*

²*CMLA, ENS Cachan, CNRS, UniverSud, 61 Avenue du Président Wilson, F-94230 Cachan, France*

PACS 05.40.+j – Fluctuation phenomena, random processes, and Brownian motion
PACS 61.43.Hv – Fractals; macroscopic aggregates (including diffusion-limited aggregates)
PACS 41.20.Cv – Electrostatics; Poisson and Laplace equations, boundary-value problems

Abstract. - Semi-permeable interfaces of irregular geometry accessed by diffusion exhibit complex transfer properties. In particular, their transfer impedance is the non trivial result of the interplay between their geometry and their physical properties. In this paper, we present a new method that we call *toposcopy*. Its aim is to solve the “inverse impedance spectroscopy problem”, namely to retrieve the geometrical features of an irregular interface from a “black box” measurement of its transfer impedance only. From previous studies, one knows that all the possible information about the geometry of an interface that can be extracted from a measurement of its impedance consists in its *harmonic geometrical spectrum*, a set of spectral characteristics of the Dirichlet-to-Neumann operator of the same interface. Here, we first describe how the toposcopy technique permits to retrieve the main components of the harmonic geometrical spectrum and to deduce from them characteristic geometrical features of the interface. The toposcopy is then tested numerically for several irregular interfaces of either simple or complex shape. It is finally shown that this method gives access to the characteristic lengths of these interfaces and, when these lengths are sufficiently different, allows to separate and quantify their respective contributions to the interface impedance.

Introduction. – The problem of transfer across irregular interfaces driven by Laplacian fields is a fundamental theoretical frame for systems in many different fields: electrochemistry [1–3], heterogeneous catalysis [4–8], NMR relaxation in porous media [9, 10], transfer across biological membranes [11], . . . In each of these situations, the physical transport properties of the system (through the bulk and across the interface) interplay in a complicated way with the geometrical characteristics of the interface, to give rise to a non trivial macroscopic response. A number of theoretical [12–18], numerical [19–21] and experimental [22, 23] works have been devoted this problem. The most common physical representation one can think of is the following: a “species” characterized by its concentration C is emitted from a distant source and diffuses into the bulk towards a “semi-permeable” interface, on which it disappears at a given rate (either by transferring across this interface, or by reacting in the case of a catalytic cell). Such a model can be put into the simple mathematical

frame:

$$\begin{cases} C = C_0 & \text{on the source} \\ \Delta C = 0 & \text{in the bulk} \\ \frac{\partial C}{\partial n} = \frac{C}{\Lambda} & \text{at the surface} \end{cases} \quad (1)$$

$\partial/\partial n$ being the normal derivative at the surface directed towards the bulk. Apart from the characteristics of the system geometry, Λ is the only parameter entering the equations. It is homogeneous to a length and is the ratio between the bulk diffusion coefficient D and the surface permeability W : $\Lambda = D/W$. In other words, in this simplified scheme of the diffusive transport across a semi-permeable interface, all the physical information about the system is condensed into the ratio of both transport parameters D and W . Knowing the geometry of the interface, one then should be able to deduce the transport properties of the system. This problem has been tackled first

by introducing the discrete Brownian self-transport operator [12, 15, 17]. Recently, a complete theoretical response has been proposed in terms of the spectral properties of the Dirichlet-to-Neumann operator [18, 19].

More difficult is the inverse problem that we address in this paper: knowing the response of a system for a large range of Λ , what information can be retrieved about the geometry of the interface? In a nutshell, the net result is the following: the information that can be extracted from such a macroscopic measurement can be summed up into a *harmonic geometrical spectrum* of the interface. This spectrum is directly related to the characteristic sizes of the interface accessible to diffusing particles.

The continuous approach. – In this section, we briefly recall the main results of the continuous approach based on the Dirichlet-to-Neumann operator [18]. For a given diffusional cell Ω , this operator (called \mathcal{M}) associates to a function f defined on the working interface $\partial\Omega$ the normal derivative $\partial u/\partial n$ of the harmonic function u such that $u = f$ on $\partial\Omega$. In physical terms, the function f can be thought of as an initial distribution of “species” on the working interface that diffuse in the bulk Ω and then come back to the interface. In the vocabulary of electrochemistry, one can consider the working interface $\partial\Omega$ with a given electric charge distribution f , and the application of the operator \mathcal{M} to f provides the density of the induced electric field. The Dirichlet-to-Neumann operator is known to be a pseudo-differential self-adjoint operator with discrete positive spectrum and smooth eigenfunctions forming a complete basis of $L^2(\partial\Omega)$ [24, 25].

It has been shown that, given a domain Ω , its Dirichlet-to-Neumann operator entirely determines the macroscopic response of the working interface. In particular, the flux density across the interface, $\phi_\Lambda = \partial C/\partial n$, can be written as [18]:

$$\phi_\Lambda = (I + \Lambda\mathcal{M})^{-1}\phi_0$$

where the flux density $\phi_0(s)$ corresponds to the solution for a perfectly absorbing interface ($\Lambda = 0$), and s is the curvilinear abscissa along the interface. The diffusion admittance $Y(\Lambda)$ of the cell is proportional to the total flux Φ_Λ through the working interface:

$$Y(\Lambda) = \Phi_\Lambda/C_0, \quad \text{with} \quad \Phi_\Lambda = \int_{interface} \phi_\Lambda(s) ds$$

It can be exactly written as an infinite sum, each term corresponding to the contribution of one eigenvector \mathbf{V}_α of the Dirichlet-to-Neumann operator \mathcal{M} :

$$Y(\Lambda) = \frac{1}{DC_0} \sum_{\alpha} \frac{F_{\alpha}}{\mu_{\alpha}(1 + \Lambda\mu_{\alpha})} \quad (2)$$

in which the μ_{α} are the eigenvalues of the operator and the F_{α} are the decomposition weights of the function $\phi_0(s)$ on the eigenvectors:

$$F_{\alpha} = \frac{(\phi_0 \cdot \mathbf{V}_{\alpha})(\phi_0 \cdot \mathbf{V}_{\alpha}^*)}{(\phi_0 \cdot \mathbf{1})(\phi_0 \cdot \mathbf{1})}$$

The μ_{α} are homogeneous to the inverse of a length, while the F_{α} are homogeneous to the inverse of an area (in 3D).

The admittance $Y(\Lambda)$ embeds into one single measurement both the bulk transport towards the interface and the surface transfer across the same interface. In the case of a perfectly absorbing interface ($\Lambda = 0$), the admittance is solely determined by the bulk transport. The added contribution of the transfer across the working interface can be characterized by the difference between the total fluxes Φ_0 and Φ_Λ : $Z(\Lambda) = C_0(\Phi_0 - \Phi_\Lambda)/\Phi_0^2$. This quantity has been shown to be an *intrinsic* characteristic of the interface and is called its *effective impedance* [15]. Its spectral decomposition can be deduced from (2):

$$Z(\Lambda) = \frac{\Lambda}{D} \sum_{\alpha} \frac{F_{\alpha}}{(1 + \Lambda\mu_{\alpha})} \quad (3)$$

The explicit formula (3) allows one to infer the exact dependence of the experimental quantity $Z(\Lambda)$ as a function of the transport parameters of the problem (Λ and D). Moreover, the influence of the geometrical irregularity is *totally* captured through the spectral characteristics μ_{α} and F_{α} of the Dirichlet-to-Neumann operator \mathcal{M} . Whatever the nature of the transport phenomena (stationary diffusion, electrical transport, molecular diffusion in heterogeneous catalysis), the geometrical irregularity of the interface can be taken into account through a set of real positive numbers $\{\mu_{\alpha}, F_{\alpha}\}$. This set, which only depends on the geometry of the interface, is called the *harmonic geometrical spectrum* of the interface [18].

It is useful to recall several known properties of the harmonic geometrical spectrum [19]. When the source is placed at infinity, the first eigenmode \mathbf{V}_0 of the Dirichlet-to-Neumann operator is constant. The other eigenmodes \mathbf{V}_{α} are orthogonal to \mathbf{V}_0 and “oscillate” around zero with some “spatial frequencies” that increase with μ_{α} . The contribution of each eigenmode to the admittance is proportional to F_{α} , as defined before. The relative (dimensionless) contributions are

$$f_{\alpha} = \frac{F'_{\alpha}}{\sum_{\alpha} F_{\alpha}} \quad (4)$$

For each contributing eigenmode, the eigenvalue μ_{α} (homogeneous to the inverse of a length) corresponds to one typical length scale of variation of the harmonic measure density while f_{α} gives the intensity of this variation. This is very similar to a “Fourier transform” of the harmonic measure, the basis being here the eigenbasis of the operator M . In other words, each geometrical irregularity of the interface generates eigenmodes that contribute to the admittance, and the eigenvalues associated to these eigenmodes are directly related to the typical sizes of the irregularity of the interface.

This suggests a method that could extract from a measurement of the effective impedance $Z(\Lambda)$ the harmonic geometrical spectrum $\{\mu_{\alpha}, F_{\alpha}\}$ by using Eq. (3). We will now present this method that we call “toposcopy”.

The toposcopy: mathematical foundation. –

The aim of the toposcopy is to extract the geometrical features of an unknown semi-permeable interface using the experimental measurements of its macroscopic response. Since, for a given interface, the harmonic geometrical spectrum entirely determines the macroscopic response of the system, this aim can be achieved in two steps:

- first, one solves the *inverse problem* that consists in finding the harmonic geometrical spectrum of an unknown interface from the macroscopic response of the system. More precisely, assuming that one can measure the impedance $Z(\Lambda)$ for a certain range of values of Λ with sufficiently high accuracy, it means to invert Eq. (3).
- second, one has to interpret the harmonic geometrical spectrum in terms of the geometrical features of the interface.

In what follows, we focus our attention on the inverse problem. One can write the expression (3) as

$$Z(\Lambda) = \frac{1}{D} \int_0^{\infty} d\lambda e^{-\lambda/\Lambda} \zeta(\lambda) \quad (5)$$

$$\text{with } \zeta(\lambda) = \sum_{\alpha} F_{\alpha} e^{-\lambda\mu_{\alpha}} \quad (6)$$

This corresponds in fact to a Laplace transform representation of the effective impedance Z considered as a function of $1/\Lambda$. But instead of the harmonic geometrical spectrum which is a Dirac comb, we now manipulate a function $\zeta(\lambda)$ which is infinitely differentiable for $\lambda > 0$. The uniqueness of the inverse Laplace transform thus provides a way to find the functional representation $\zeta(\lambda)$ of the harmonic geometrical spectrum from a measurement of the macroscopic response of the system.

In principle, it should be possible to compute the whole harmonic geometrical spectrum $\{\mu_{\alpha}, F_{\alpha}\}$ containing all the information on the geometry which may be available from such an experiment. However, one should take into account a finite accuracy of the experimental measurements, errors due to the numerical inversion of the Laplace transform, difficulties to determine the spectral characteristics μ_{α} and F_{α} from function $\zeta(\lambda)$, and the *a priori* infinite number of eigenmodes. In what follows, we address these issues in detail.

The first simplification can be achieved by assuming the existence of a minimal cut-off ℓ of the geometrical irregularity. The introduction of the minimal cut-off is very reasonable and even necessary from the physical point of view: the molecular diffusion governed by the Laplace equation can be used only if the mean free path of diffusing particles is sufficiently smaller than the geometrical features of the boundary. In this case, the harmonic measure density $\phi_0^h(s)$ becomes smooth at scales smaller than ℓ , and its projection on the high-frequency oscillating

eigenfunctions $\mathbf{V}_{\alpha}(s)$ vanishes. Thus, only a finite number of eigenmodes has to be taken into account in the inversion procedure which reduces the infinite sum in Eq. (5) to a finite sum over the contributing modes.

One should note that, if the mean free path is much larger than the geometrical irregularities of the boundary, in particular in heterogeneous catalysis, the system enters another regime called *Knudsen diffusion* [26, 27]. In this situation, the molecules may enter deeply into narrow pores and their landing probabilities on the interface do not correspond anymore to the harmonic measure. The inversion method proposed in this paper would then fail in this case to detect the geometrical irregularities significantly smaller than the mean free path.

As will be shown below, the toposcopy is not intended to distinguish different features of the interface of similar sizes. The aim is more to determine the respective contributions from sizes of different orders of magnitude to the macroscopic response. In this frame, the second simplification is to assume the existence of *separated characteristic scales* in the interface (such as, e.g., in self-similar (pre)fractal boundaries). In this case, it has been shown that only *a few* eigenmodes significantly contribute to the macroscopic response of the system [17, 19]. Moreover, the associated eigenvalues correspond to the inverses of characteristic scales of the interface. In the general case of any interface, this assumption will correspond to regrouping the contributions of eigenmodes with eigenvalues relatively close to each other.

The inversion technique consists in inverting the measured impedance curve $Z(\Lambda)$ (e.g., by using Gaver-Wynn-Rho or Talbot algorithms [28]) and looking for $\zeta(\lambda)$ as a finite sum of exponentials with well-separated parameters μ_{α} [29]. This procedure will give as a result a sequence $\{\hat{\mu}_k, \hat{F}_k\}$ which is an approximate solution of the original problem (after cut-off and possible regrouping of the contributing eigenmodes).

To summarize, the toposcopy extracts from a direct measurement of the effective impedance curve the approximate harmonic geometrical spectrum $\{\hat{\mu}_k, \hat{F}_k\}$. The eigenvalues $\hat{\mu}_k$ are the inverses of the characteristic variation lengths of the harmonic measure on the interface. These characteristic lengths are in direct correlation with the characteristic scales of the interface itself. In turn, the factors \hat{F}_k represent the relative contributions of these scales to the macroscopic impedance.

Numerical validation. – In order to check the applicability of the toposcopy, we consider various interfaces: simple curves with one or two different irregularities, and deterministic and random Koch curves.

For each interface, we perform the following computation:

- first, the boundary element method is used to compute the spectral characteristics of the Dirichlet-to-Neumann operator, allowing one to express the effective impedance $Z(\Lambda)$ according to Eq. (3).

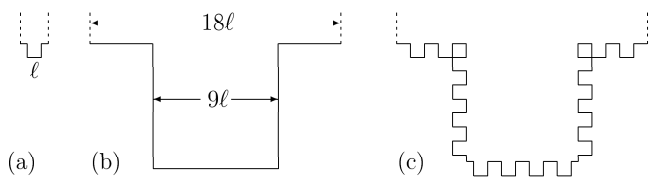


Fig. 1: Three simple curves to test the toposcopy: (a) a small pore; (b) a large pore (nine times larger than ‘a’); (c) a large pore “decorated” by small pores. Diffusing particles arrive from an infinitely distant source located above. The dotted vertical lines (with periodic boundary condition) delimit the bulk region.

- second, we apply the toposcopy technique to extract from the effective impedance curve $Z(\Lambda)$ alone the approximate values of $\hat{\mu}_k$ and \hat{F}_k . This is realized without any *a priori* knowledge of the interface. Thus, the impedance curve could as well come from a real experiment providing the macroscopic response of a system with “unknown” geometry.
- finally, one compares the obtained values of $\hat{\mu}_k$ and \hat{F}_k with the initial harmonic geometrical spectrum $\{\mu_\alpha, F_\alpha\}$ and the typical sizes of the interface irregularities.

Interfaces with two characteristic pore sizes. We first test the toposcopy technique on three simple interfaces in 2D. These interfaces are represented in Fig. 1: first, a square pore; second, its copy magnified by a factor 9; third, the same copy but now “decorated” with smaller square pores analog to the first interface, such that the average width of the large pore is still 9ℓ . While the first two curves are intended to represent “elementary” (one-scale) geometrical features, the latter curve has irregularities at two different scales.

Figure 2 presents the effective impedances of the three interfaces as a function of the parameter Λ . One can notice that, from the impedance curve only, the interfaces (b) and (c) may be barely distinguishable within the measurement errors. Figure 3 shows the harmonic geometrical spectra $\{\mu_\alpha, F_\alpha\}$ extracted using the toposcopy technique.

In all cases, the lowest eigenvalue (which is the closest to 0) corresponds to the inverse of the effective distance between the interface and the distant source [18]. In our simulations, the source was placed at infinity, yielding $\mu_0 = 0$. The contribution F_0 of this eigenvalue is equal to the inverse of the total perimeter of the interface. Since these data do not carry any information about the typical sizes of the interface irregularities, we will from now only consider the other contributions.

In the two first cases (a) and (b), one observes only one contributing peak located at $\mu_1^a \simeq 1.038$ for the small pore (a) and at $\mu_1^b \simeq 0.115$ for the large pore (b) (the eigenvalues are expressed in units of ℓ^{-1} , ℓ being the width of the small pore (a)). The inverses of μ_1^a and μ_1^b (respectively,

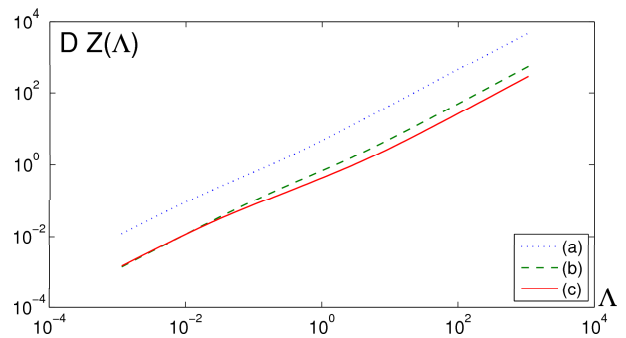


Fig. 2: (Color online). The effective impedance for three simple curves shown in Fig. 1.

0.96 and 8.67) then provide the typical irregularity sizes of both pores, as “seen” by diffusing particles.

The third curve represents the pore (b) “decorated” by the small pores (a). One now observes two contributing peaks at $\mu_1^c \simeq 0.055$ and $\mu_2^c \simeq 0.786$ which lead respectively to the lengths 18.18 and 1.27. The smaller length corresponds to the size of the small pore (a), while the larger corresponds to twice the size of the pore (b). This factor 2 is the ratio between the perimeters of the interfaces (c) and (b).

The toposcopy technique thus allows in this case to identify and separate the characteristic length scales of the interface, which were “hidden” in the impedance curve.

Deterministic Koch boundaries. Prefractal boundaries, which exhibit irregularity at various scales, can be used as test geometries for the toposcopy technique. We first consider the deterministic quadratic Koch curve of fractal dimension $D_f = \ln 5 / \ln 3$ (the third generation of this curve is shown on the left of Fig. 4).

Numerical simulations carried out in [17, 19] show that the harmonic geometrical spectrum of the generation g of this curve presents mainly $(g + 1)$ eigenmodes contributing to the impedance, while the contribution of the other eigenmodes can be neglected. For example, this spectrum for the third generation is drawn on Fig. 5.

One can now compare the exact harmonic geometrical spectrum $\{\mu_\alpha, F_\alpha\}$ to the set $\{\hat{\mu}_\alpha, \hat{F}_\alpha\}$ deduced from the impedance curve by using the toposcopy technique (Fig. 5). In both sets, the contribution of the lowest eigenmode $\mu_0 = 0$ corresponds to the ratio between the diameter L of the interface and its developed perimeter. The toposcopy gives the exact value $0.216 = (3/5)^3$. The exact harmonic geometrical spectrum presents three other main peaks surrounded by a collection of eigenmodes of much smaller contributions. The application of the toposcopy technique to the impedance response allows one to retrieve the same three peaks. Their intensities are comparable but not identical to the original intensities of the harmonic geometrical spectrum, because the peaks deduced from the toposcopy also contain the contributions of the surrounding eigenmodes. The toposcopy technique produces two

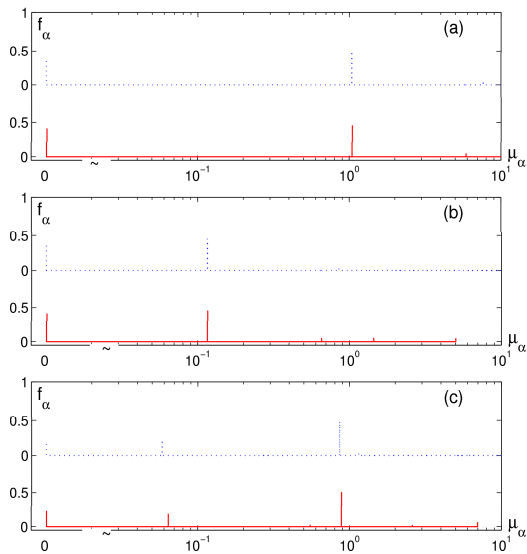


Fig. 3: (Color online). The harmonic geometrical spectra for three simple curves shown in Fig. 1. To present the eigenvalue $\mu_0 = 0$ at logarithmic scale, the abscissa axis is interrupted. The contributing peaks computed by the toposcopy technique are shown below each harmonic geometrical spectrum. For the curves (a) and (b), the toposcopy technique retrieves the mean contributing peaks with a very high accuracy (the recovered peaks are barely distinguishable from the original ones). In the case of the “decorated” curve (c), one can also distinguish the peaks corresponding to the two typical lengths of the interface.

spurious peaks (at $\mu \simeq 50$ and $\mu \simeq 136$) which in fact gather the contributions of all high frequency eigenmodes. The corresponding lengths μ^{-1} of the three main peaks ($\mu = 0.65$, $\mu = 3.44$, and $\mu = 19.67$) are 1.54, 0.29, 0.05, respectively. This shows that the interface presents characteristic irregularities at each of these scales.

Thus, the toposcopy technique allows one to extract the harmonic geometrical spectrum, from which one can then recover the characteristic scales of the geometry and their relative weights.

In order to check the quality of this technique, one can now reconstruct the effective impedance $Z(\Lambda)$ by using the data $\{\hat{\mu}_k, \hat{F}_k\}$ computed by toposcopy. The maximal relative error is found to be of order of 10^{-3} .

Random Koch boundaries. The deterministic Koch boundaries provide an example of an irregular interface with well-defined characteristic scales. However, in general, real interfaces do not present a perfect hierarchical structure. In order to study a more realistic case, one considers random Koch boundaries (one realization of this curve is shown on the right of Fig. 4).

Using the same approach as for the previous interfaces, one determines from the impedance response the values of $\hat{\mu}_k$ and \hat{F}_k (Fig. 5). Once again, the position and the contribution of the lowest eigenmode ($\mu_0 = 0$) is found with good accuracy. The first eigenmode with nonzero

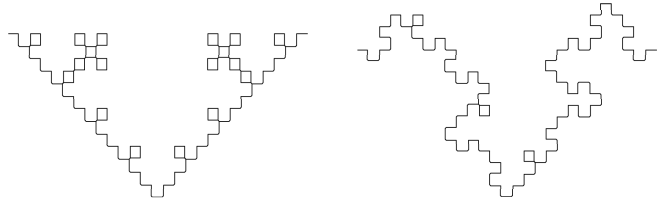


Fig. 4: The test geometries: third generation of the deterministic (left) and random (right) Koch curves.

eigenvalue μ is also extracted with a very good precision. For the higher frequency eigenmodes, one can see that the toposcopy technique gives a simplified harmonic geometrical spectrum by regrouping modes of comparable eigenvalues. Thus, this technique is not meant to separate very similar characteristic sizes of the interface, as for instance two characteristic lengths in a ratio 2:1. This is not surprising since the impedance responses $Z(\Lambda)$ of deterministic and random prefractal interfaces of the same fractal dimension and same generation are known to be almost indistinguishable [30]. In a few words, the toposcopy technique is really a tool designed to deduce from impedance measurements the characteristic variation lengths of the harmonic measure on the interface and from them, for each order of magnitude, the typical sizes of the interface and their relative contributions to the overall transfer response.

It is interesting to note that, although their impedance curves are very similar, the harmonic geometrical spectra of both deterministic and random interfaces extracted by toposcopy are not identical. In that sense, the toposcopy, which is mathematically the natural way to solve the inverse problem, acts as a “magnifying glass” by enhancing the tiny differences between the impedance curves.

Conclusion. — In this paper, we addressed the inverse problem consisting in retrieving, from impedance measurements, the geometry of an interface accessed by a Laplacian current. More precisely, the main question was: “Which information about the geometrical features of the interface can be extracted from experimental measurements of the macroscopic response of the system?” One knows from previous works that this information is all contained in the harmonic geometrical spectrum $\{\mu_\alpha, F_\alpha\}$ of the interface, namely the spectral decomposition of the harmonic measure onto the eigenbasis of the Dirichlet-to-Neumann operator. In theory, the absolute knowledge of the impedance response should allow a complete determination of this harmonic geometrical spectrum.

The inversion technique presented here, called toposcopy, allows in fact to identify the orders of magnitude of the main contributing eigenvalues. In turn, these eigenvalues correspond to the typical feature sizes of the interface. For interfaces with precisely defined and separated length scales (as for instance a determin-

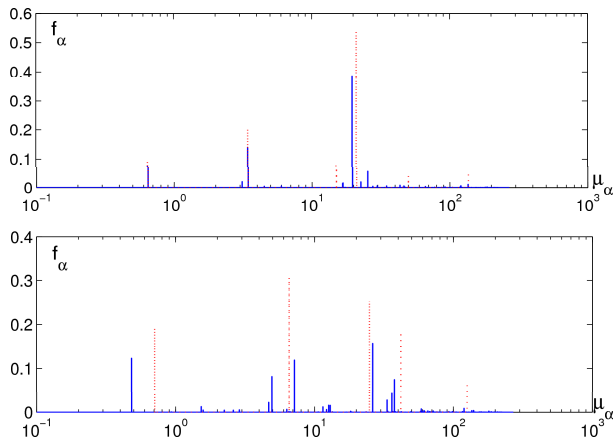


Fig. 5: (Color online). (top) The harmonic geometrical spectrum of the third generation of the deterministic quadratic Koch curve (the zeroth eigenmode with $\mu_0 = 0$ is not present on the log-scale). The dotted lines show the contributing peaks determined by the toposcopy technique. (bottom) The harmonic geometrical spectrum of the third generation of the random Koch curve. The dotted lines show the contributing peaks determined by the toposcopy technique.

istic prefractal interface), it has been shown that the toposcopy technique even retrieves accurately the exact positions and amplitudes of the main contributing peaks. In practical applications such as in electrochemistry for which a large range of parameter Λ can be explored by varying the frequency of the applied electric potential, the toposcopy technique would extract informations for the characteristic lengths of the interface. In other fields, the exploration range would be more limited, but the toposcopy could still be used to extract informations for this reduced range of lengths.

In summary, this technique permits, at least in theory, to deduce from a macroscopic measurement qualitative and quantitative characteristics of a transfer interface. It may have direct applications in systems driven by Laplacian field (diffusion, NMR, electrochemistry, catalysis), for which the transfer interface at work may be difficult to observe visually.

Acknowledgments. — We wish to thank Bernard Sapoval for fruitful discussions and advices. We would like to thank the ANR for its financial support through the project MIPOMODIM, ANR NT05-1.42030.

REFERENCES

[1] R. de Levie, *Electrochimica Acta* **10**, 113-130 (1965).
 [2] S. H. Liu, *Phys. Rev. Lett.* **55**, 529-532 (1985).
 [3] L. Nyikos, T. Pajkossy, *Electrochimica Acta* **30**, 1533-1540 (1985).
 [4] G. F. Froment, K. B. Bischoff, *Chemical Reactor Analysis and Design* (Wiley, New York, 1990).

[5] J. M. Thomas, W. J. Thomas, *Principles and Practice of Heterogeneous Chemistry* (VCH, Weinheim, 1997).
 [6] T. Elias-Kohav, M. Sheintuch, D. Avrin, *Chem. Engng. Sci.* **46**, 2787 (1991).
 [7] R. Gutfraind, M. Sheintuch, D. Avnir, *J. Chem. Phys.* **95**, 6100-6111 (1991).
 [8] M.-O. Coppens, *Catal. Today* **53**, 225 (1999).
 [9] P.-G. de Gennes, *Comptes. Rendus Acad. Sc., série II* **295**, 1061 (1982).
 [10] K. R. Brownstein, and C. E. Tarr, *Phys. Rev. A* **19** (6), 2446-2453 (1979).
 [11] Sapoval, B., In: Nonnenmacher, T.F., Losa, G.A., Weibel, E.R. (Eds.). *Fractals in Biology and Medicine*. Birkhäuser-Verlag, Bâle (1994).
 [12] T. C. Halsey, *Phys. Rev. A* **35**, 3512 (1987).
 [13] T. C. Halsey, M. Leibig, *Annals of Physics* **219**, 109 (1992).
 [14] B. Sapoval, *Phys. Rev. Lett.* **73**, 3314 (1994).
 [15] M. Filoche, B. Sapoval, *Eur. Phys. J. B* **9**, 755-763 (1999).
 [16] M.H.A.S Costa, A.D. Araujo, H.F. da Silva, J.S. Andrade Jr, *Phys. Rev. E* **67**, 061406 (2003).
 [17] D. S. Grebenkov, M. Filoche, B. Sapoval, *Eur. Phys. J. B* **36**, 221-231 (2003).
 [18] D. S. Grebenkov, M. Filoche, B. Sapoval, *Phys. Rev. E* **73**, 021103 (2006).
 [19] D. S. Grebenkov, M. Filoche, B. Sapoval, *Fractals* **15**, 27-39 (2007).
 [20] M. Leibig and T.C. Halsey, *J. Electroanal. Chem.* **358**, 77 (1993).
 [21] H. Ruiz-Estrada, R. Blender, W. Dieterich, *J. Phys.: Condens. Matter* **6**, 10509-10517 (1994).
 [22] M. Keddad, H. Takenouti, *Electrochimica Acta* **33**, 445 (1988).
 [23] A. Le Mehaute, G. Crepy, *Solid State Ionics* **9&10**, 17 (1983).
 [24] M. S. Agranovich, in *Partial Differential Equations IX*, Ed. by M. S. Agranovich, Yu. V. Egorov, M. S. Shubin, EMS 79 (Springer, 1997).
 [25] M. S. Birman, M. Z. Solomyak, *Spectral Theory of Self-Adjoint Operators in Hilbert Space* (D.Reidel Publishing Company, 1987).
 [26] K. Malek, M.-O. Coppens, *Phys. Rev. Lett.* **87**, 125505 (2001).
 [27] J. S. Andrade jr., H. F. de Silva, M. Baquil, B. Sapoval *Phys. Rev. E* **68**, 041608 (2003)
 [28] J. Abate, P. P. Valkó, *Int. J. Numer. Meth. Engng.* **60**, 979-993 (2004).
 [29] G. Beylkin, L. Monzón, *Appl. Comput. Harmon. Anal.* **19**, 17 (2005).
 [30] M. Filoche, B. Sapoval, *Phys. Rev. Lett.* **84**, 5776 (2000).